# Dominant Role of Quantum Anharmonicity in the Stability and Optical Properties of Infinite Linear Acetylenic Carbon Chains

Davide Romanin, Lorenzo Monacelli, Raffaello Bianco, Ion Errea, Francesco Mauri, Matteo Calandra

## To cite this version:

Davide Romanin, Lorenzo Monacelli, Raffaello Bianco, Ion Errea, Francesco Mauri, et al.. Dominant Role of Quantum Anharmonicity in the Stability and Optical Properties of Infinite Linear Acetylenic Carbon Chains. Journal of Physical Chemistry Letters, 2021, 12 (42), pp.10339 - 10345. 10.1021/acs.jpclett.1c02964 . hal-03407561

HAL Id: hal-03407561
https://hal.sorbonne-universite.fr/hal-03407561v1

Submitted on 29 Oct 2021

# Dominant Role of Quantum Anharmonicity in the Stability and Optical Properties of Infinite Linear Acetylenic Carbon Chains

| | |
|---|---|
| Journal: | *The Journal of Physical Chemistry Letters* |
| Manuscript ID | jz-2021-02964d.R2 |
| Manuscript Type: | Letter |
| Date Submitted by the Author: | 12-Oct-2021 |
| Complete List of Authors: | Romanin, Davide; Institut des NanoSciences de Paris, CNRS<br>Monacelli, Lorenzo; Universita degli Studi di Roma La Sapienza, Physics Department<br>Bianco, Raffaello; Centro de Fisica de Materiales<br>Errea, Ion; Centro de Fisica de Materiales<br>Mauri, Francesco; University of Rome La Sapienza, Department of Physics<br>Calandra, Matteo; Università degli Studi di Trento, Departement of Physics |
| | |

# Dominant Role of Quantum Anharmonicity in the Stability and Optical Properties of Infinite Linear Acetylenic Carbon Chains

Davide Romanin,[*,†] Lorenzo Monacelli,[‡] Raffaello Bianco,[¶] Ion Errea,[¶,§]
Francesco Mauri,[‡] and Matteo Calandra[*,‖,†]

†*Sorbonne Université, CNRS, Institut des Nanosciences de Paris, UMR7588, F-75252, Paris, France*

‡*Dipartimento di Fisica, Universitá di Roma La Sapienza, Piazzale Aldo Moro 5, I-00185 Roma, Italy*

¶*Centro de Física de Materiales (CSIC-UPV/EHU), Manuel de Lardizabal pasealekua 5, 20018 Donostia-San Sebastián, Basque Country, Spain*

§*Fisika Aplikatua 1 Saila, Gipuzkoako Ingeniaritza Eskola, University of the Basque Country (UPV/EHU), Europa Plaza 1, 20018, Donostia San Sebastián, Basque Country, Spain*

‖ *Department of Physics, University of Trento, Via Sommarive 14, 38123 Povo, Italy*

E-mail: romanin@insp.jussieu.fr; m.calandrabuonaura@unitn.it

## Abstract

Carbyne, an infinite-length straight chain of carbon atoms, is supposed to undergo a second order phase transition[1] from the metallic bond-symmetric cumulene $(=\mathrm{C}=\mathrm{C}=)_\infty$ towards the distorted insulating polyyne chain[2] $(\text{-C}\equiv\text{C-})_\infty$ displaying bond-length alternation. However, recent synthesis of ultra long carbon chains ($\sim 6000$ atoms)[3–5] did not show any phase transition and detected only the polyyne phase, in agreement with previous experiments on capped finite carbon chains.[6,7] Here, by performing first principles calculations, we show that quantum-anharmonicity reduces the energy gain of the polyyne phase with respect to the cumulene one by 71%. The magnitude of the bond-length alternation increases by increasing temperature, in stark contrast with a second order phase transition,[1] confining the cumulene-to-polyyne transition to extremely high and unphysical temperatures. Finally, we predict that a high temperature insulator-to-metal transition occurs in the polyyne phase confined in insulating nanotubes with sufficiently large dielectric constant due to a giant quantum-anharmonic bandgap renormalization.

# Graphical TOC Entry

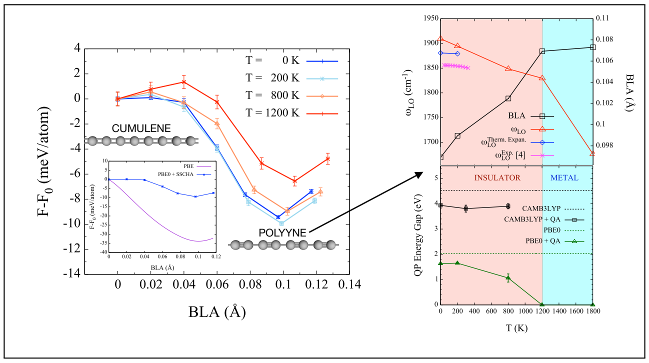

Charge density waves (CDW) are broken symmetry states in solids in which the crystal acquires a periodic modulation of a given wavevector at low temperature. They are ubiquitous as they occurs in many different systems ranging from high-Tc superconductors,[8] transition metal dichalcogenides,[9] 2D materials[10–12] and one dimensional systems.[2,13] The understanding of this phenomenon is difficult as it is determined by the interplay of three effects: the electron-electron interaction, the electron-phonon coupling and quantum anharmonicity. On a general basis, the electron-phonon interaction enhances the tendency towards CDW while quantum anharmonicity suppresses it.[14–16] Nevertheless, few estimates of the magnitude of quantum anharmonicity are present in literature[14–16] mostly because of its non-perturbative nature. Moreover, in the case of light atoms, the quantum nature of the ions is crucial and difficult to treat with conventional density functional theory (DFT) [17] or standard molecular dynamics approaches.

Linear acetylenic carbon, or carbyne,[18] is considered the physical realization of a one dimensional CDW. Therefore, the understanding of the finite temperature phase diagram of this system and the comprehension of the mutual role of the relevant interactions (electron-phonon, electron-electron and quantum anharmonicity) is of paramount importance. Historically,[1,2] the cumulene-to-polyyne transition was attributed to the electron-phonon interaction and the perfect nesting condition at $2k_F$ in cumulene, leading to a divergence in the real part of the charge-charge response function at $T = 0$ K. This consequent large single particle energy gain due to gap opening should stabilize the polyyine phase. However, this hipothesis, valid in the small displacements regime, is unlikely.

Several density functional theory based calculations (neglecting quantum anharmonicity) showed a band-gap opening larger than 2 eV (see Tab. 1), with a total energy gain of the polyyne phase with respect to the cumulene one smaller than 150 meV.[19] Moreover, the bond-length alternation (BLA), defined as the length difference between the single ($r_1$) and the triple ($r_3$) bonds of polyyne, is found to be substantial and ranging between $0.09 - 0.14\mathring{A}$ (corresponding to $7 - 10\%$ of the average bond length of polyyne). These structural distortions from the ideal cumulene phase are definitely not in the small displacement limit. Still one would expect that raising temperature the BLA should progressively reduce, as it happens in a second order phase transition, and the cumulene phase becomes stable at some critical temperature $T_{CDW}$. This argument, however, does not account for quantum-anharmonicity, whose magnitude and temperature dependence are still largely unexplored in literature. Moreover, the experimental data are in stark disagreement with the occurrence of a cumulene-to-polyyne phase transition as at any temperature cumulene observations are very rare (and mostly related to strain and charging effects[20–22]), while polyyne has been obtained either in relatively small (up to $\sim 44$ atoms) end-capped chains[6,7,23] or through encapsulation in single-,[24,25] double-[4,26] and multi-walled[27] carbon nanotubes, with chains as long as $\sim 6000$ atoms.

In this work we investigate the ground state and the CDW transition of infinite carbon chains by using hybrid functionals, self-consistent GW, the Bethe-Salpeter equation and by including quantum anharmonicity within the Stochastic Self-Consistent Harmonic Approximation (SSCHA).[17,28–30] We show that quantum anharmonicity completely reshapes the stability of the different carbyne phases, reducing the energy difference between the polyyne and cumulene phase by 71%. Even more surprisingly, we show that the BLA *increases* by *increasing* temperature, the opposite of what is expected in a second order phase transition. Finally, we demonstrate that quantum-anharmonic effects on optical properties are extremely large and strongly temperature dependent.

In order to do so, density functional theory (DFT) calculations are performed both with the plane-wave pseudopotential method, using the Perdew-Burke-Ernzerhof (PBE) exchange-correlation (xc) functional and Quantum ESPRESSO,[31,32] and with localized gaussian basis, using both the PBE0 and CAMB3LYP hybrid xc functionals and CRYSTAL.[33,34] In the Quantum ESPRESSO code we use a norm-conserving pseudopotential, while in the CRYSTAL code we use the triple-$\xi$-polarized Gaussian type basis set.[35] Quantum anharmonicity is taken into account via the stochastic self-consistent harmonic approximation

(SSCHA),[17,28–30] for which we use the CRYSTAL[33,34] code as force engine: forces and energies are computed on supercells with 20 atoms per unit cell, containing the unstable phonon mode. Optical properties of the distorted phase are computed within the self-consistent GW approximation on eigenvalues only (ev$GW$) using the Yambo[36,37] code within the plasmon-pole approximation.[38] Excitonic effects for the freestanding carbon chain are then evaluated by solving the Bethe-Salpeter[39,40] equation (BSE) on top of the ev$GW$ band structure. More details concerning computational methods can be found in the Supporting Informations.

A large number of first-principles calculations have been performed on linear carbon chains of both finite and infinite size, however almost all of them neglect quantum anharmonicity and its temperature dependent effects as well as its interplay with electron-electron interaction. The calculated quasiparticle band gap as well as the BLA value are strongly dependent on the assumptions employed to model electron-electron interaction[41–45] (Tab. 1). The best results with respect to more accurate treatments of electronic correlation (e.g. quantum Monte Carlo[45] or RPA[46]) for carbyne in vacuum are obtained via DFT and partial inclusion of the exact exchange from Hartree Fock (HF), as parametrized in hybrid functionals with unscreened long range exchange such as CAMB3LYP[42–44] (see the inset of Fig. 3 (a) and Sec. S4 in the SI). However, even if the PBE0 hybrid functional gives a slightly reduced BLA in vacuum, its value is very close to that of very long carbon chains inside the dielectric environment of the carbon nanotube[46] (see Tab. 1, as well as Sec. S4 in the SI). Indeed, the BLA is expected to strongly depend on the environment around the carbyne chain. For this reason, and to better compare with experiments, in the following we adopt the CAMB3LYP functional to model carbyne in vacuum and PBE0 to describe carbyne in the presence of the dielectric environment of the nanotube.[47]

**Table 1: Structural, optical and vibrational properties of carbyne for different exchange correlation functionals with and without quantum anaharmonic (QA) effects. The column $n$ shows if the calculation is obtained on an infinite system with periodic boundary conditions (PBC) or on chains of finite size of length $n$. The subsequent four columns are used to describe the accuracy of the computational methods: *MF* refers to a mean-field approach, *X* and *C* are used to signal a more accurate treatment for electronic exchange interaction and correlation respectively, while *QA* indicates if quantum nuclear fluctuations are taken into account. The polyyne lattice parameter is labeled $2c$, while $r_1$ and $r_3$ are the single and triple bond lengths, respectively. The bond length alternation (BLA)is defined as $r_3 - r_1$. Finally $\Delta E$ and $\omega_{LO}$ represents the quasiparticle energy bandgap and the longitudinal optical frequency at the zone center, respectively.**

| Method | n | MF | X | C | QA | 2c (Å) | $r_1$ (Å) | $r_3$ (Å) | BLA (Å) | $\Delta E$ (eV) | $\omega_{LO}$ (cm$^{-1}$) |
|---|---|---|---|---|---|---|---|---|---|---|---|
| This work | | | | | | | | | | | |
| DFT-PBE0 | PBC | ● | ● | | | 2.534 | 1.3156 | 1.2183 | 0.0973 | 2.03 | 1986.57 |
| DFT-CAMB3LYP | PBC | ● | ● | | | 2.526 | 1.3286 | 1.1973 | 0.1313 | 4.39 | 2277.22 |
| DFT-PBE0 + QA | PBC | ● | ● | | ● | 2.534 | 1.3154 | 1.2185 | 0.0969 | 1.63 (0 K) | 1909.3 |
| DFT-CAMB3LYP + QA | PBC | ● | ● | | ● | 2.526 | 1.3304 | 1.1955 | 0.1348 | 3.94 (0 K) | 2226.5 |
| evGW@PBE0 | PBC | | ● | ● | | 2.534 | 1.3154 | 1.2185 | 0.0969 | 3.21 | - |
| evGW@CAMB3LYP | PBC | | ● | ● | | 2.526 | 1.3304 | 1.1955 | 0.1348 | 4.32 | - |
| Literature | | | | | | | | | | | |
| DMC[45] | PBC | | ● | ● | | 2.5817(9) | 1.359(2) | 1.223(2) | 0.136(2) | 3.4(1) | 2084(5) |
| DMC+ZPE on $\Delta E$[45] | PBC | | ● | ● | | 2.5817(9) | 1.359(2) | 1.223(2) | 0.136(2) | 3.3(0) | - |
| RPA (vacuum)[46] | PBC | ● | ● | ● | | 2.590 | 1.36 | 1.23 | 0.129 | - | 2000 |
| RPA (nanotube)[46] | PBC | ● | ● | ● | | 2.590 | 1.3405 | 1.2495 | 0.091 | - | 1614 |
| HF[42] | 72 | ● | ● | | | - | - | - | 0.183 | 8.500 | - |
| MP2[42] | 40 | | ● | ● | | - | - | - | 0.060 | 5.541 | - |
| MP2[41] | PBC | | ● | ● | | 2.554 | 1.337 | 1.217 | 0.120 | - | - |
| CCSD(T)[48] | 36 | | ● | ● | | - | - | - | 0.125 | - | 2090 |
| CCSD(T)[41] | PBC | | ● | ● | | 2.565 | 1.358 | 1.207 | 0.151 | - | - |
| DFT-LDA[41] | PBC | ● | | | | 2.532 | 1.286 | 1.246 | 0.040 | - | - |
| DFT-PBE[45] | PBC | ● | | | | 2.565 | 1.300 | 1.265 | 0.035 | - | - |
| DFT-HSE06[45] | PBC | ● | ● | | | 2.56 | 1.323 | 1.237 | 0.086 | - | - |
| DFT-B3LYP[42] | 72 | ● | ● | | | - | - | - | 0.088 | 1.487 | - |

The role played by quantum effects on the BLA is still undisclosed. The zero point energy contribution to the free energy is larger than the energy gain between the cumulene and polyyne structures.[19] The only existing calculation performed by including to some extent quantum anharmonicity confirms this argument and shows that polyyne is not anymore stable if a semilocal fucntional (PBE) is used as force engine,[19] in qualitative disagreement with experiments and again pointing to the crucial role of quantum anharmonicity and electron-electron interaction. However, PBE is known to be largely inaccurate for carbyne as it underestimates the BLA by ≈ 75% with respect to quantum Monte Carlo simulations (Tab. 1).

The relative stability of the cumulene and polyyne phases inside CNTs as a function of temperature can be determined by calculating the quantum free energy in the SSCHA as a function of the BLA (Fig. 1 and Sec. S2 in the SI) using PBE0. At $T = 0$, cumulene is unstable towards polyyne. The quantum total energy difference is ≈ 9 meV/atom, while the classical total energy difference (reported in the inset of Fig. 1) is ≈ 34 meV/atom. The comparison between these two results highlights the crucial role of quantum anharmonicity leading to a 71% suppression of the energy gain by the distortion (a reduction of 25 meV/atom). If quantum anharmonicity is neglected, the phase stability of polyyne is significantly overestimated.

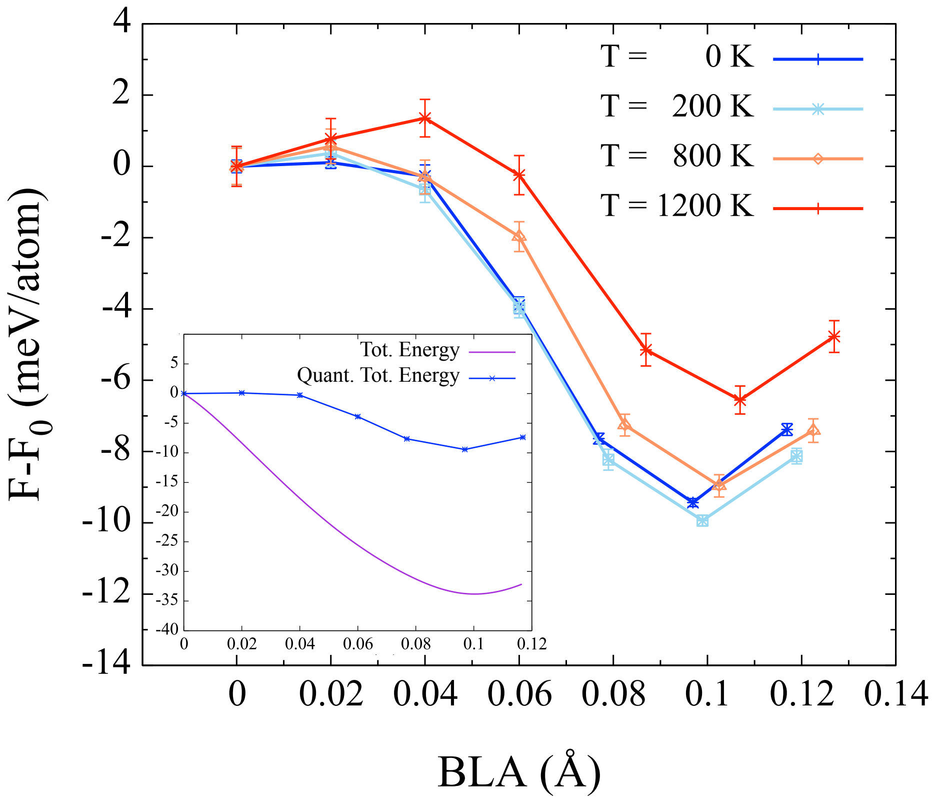

Figure 1: **First-order phase transition in carbyne.** a) Quantum anharmonic free energy difference per carbon atom between the polyyne and cumulene phases as a function of the bond length alternation (BLA) and temperature. The inset shows the comparison between the total energy difference and the quantum free energy difference at $T = 0$ between the two phases as a function of the BLA.

As temperature is raised, cumulene becomes metastable, with a small local minimum in the quantum free energy at BLA$=0$ (Fig. 1) that occurs for $T > T_P \approx 75$K (see Sec. S2.4 in SI for the estimate of $T_P$). This metastable minimum is the one described by the Peierls theory at high temperature (i.e. stabilization of the the cumulene phase by temperature). As $T$ approaches $T_P$ from above, the free energy curvature at zero BLA is reduced, becomes zero at $T = T_P$ and negative below, as it happens in a prototypical second order phase transition (see also Fig. S9 in the SI). However, this minimum is, by far, not the global minimum of the free energy curve that occurs at large finite BLA values of the order of $\approx 0.1$Å . Even at temperatures as large as 1200 K, the quantum free energy calculation shows that polyyne is the most stable phase with an energy gain with respect to cumulene of $\approx 6$ meV per atom. The transition between the two structures occurs at extremely high and unphysical temperatures (extrapolated to $\approx 3500$ K whithin PBE0, see SI Sec. S2.5). Our calculation explains why only polyyne is always detected in experiments and not cumulene, even at very high temperatures.[4,6,7,24–27]

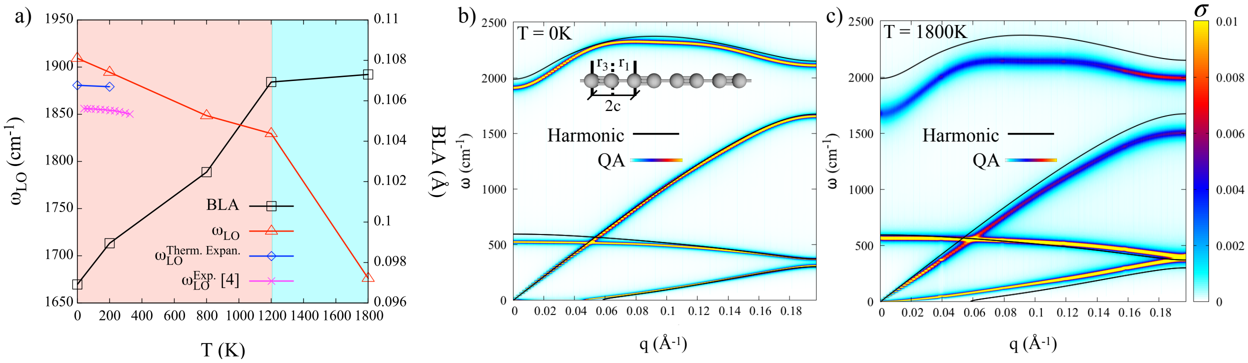

Figure 2: **Vibrational properties of polyyne.** a) Bond length alternation and longitudinal optical phonon frequency (including quantum anharmonic effects) for the polyyne phase as a function of temperature: $\omega_{LO}^{Exp.}$, $\omega_{LO}$ and $\omega_{LO}^{Therm.Expan.}$ are the experimental[4] and theoretical longitudinal phonon frequencies at fixed and relaxed lattice parameters (for more details see Sec. S2.6 in the SI) b)-c) Harmonic (black solid line) and quantum anharmonic (color map) phonon dispersion relation of polyyne at $T = 0$ K (c) and $T = 1800$ K (d) The color bar represents the magnitude of the phonon cross-section $\sigma$ (Eq. S7).

Finally, we remark that in a second order CDW phase transition, the magnitude of the order parameter (BLA) should decrease as temperature increases and, ultimately, becomes zero at and above the CDW transition. In the case of polyyne the opposite occurs, namely the BLA *increases by increasing temperature* up to $\approx$ 1200K (Fig. 2 (a)) and ultimately it saturates above 1200 K due to the occurrence of an unexpected insulator-to-metal transition driven by quantum anharmonic effects (see later). We underline that the results in Fig. 2 (a) (black line) for the BLA have been obtained by performing the full quantum anharmonic optimization of the internal coordinates at fixed cell.

The phonon dispersions of polyyne are shown in Fig. 2 (b)-(c), both in the harmonic approximation (black solid line) and by including dynamical effects in the anharmonic phonon spectral weight (color maps, see Sec. S2.1 of SI and Ref.[30] for more details). In the static case, quantum anharmonicity lowers the energy of the longitudinal optical mode (Fig. S6 (a) ). However, dynamical effects in the phonon spectral weight enhance the quasiparticle energies with respect to the static case both of optical and acoustic modes, as shown in Fig. 2 (b)-(c) (see also Sec. S2.3 in the SI). Finally, the dependence on temperature of the dynamical phonon frequency of the longitudinal optical Raman-active mode at fixed cell is reported in Fig. 2 (a) and in Tab. 1. The phonon frequency decreases linearly with temperature up to the insulator-to-metal transition at $\approx$ 1200 K. At $T = 0$ ($T = 800$K) the blueshift of the Raman active mode due to quantum anharmonicity is $\approx 77$ cm$^{-1}$ ($\approx 137$ cm$^{-1}$), namely approximately 4% (7%) of the harmonic PBE0 phonon frequency.

In the $0 - 200$ K temperature range, where experimental data are available,[4] we perform the complete quantum anharmonic optimization of the crystal structure to account for the thermal expansion. Going from 0 to 200 K, Carbyne tends to contract by increasing temperature (see SI Sec. 2.6) which affects the temperature dependence of the longitudinal optical phonon frequency. If the (negative) thermal expansion is included, the behaviour of the longitudinal optical phonon frequency versus temperature is in good agreement with available experimental data, as shown in Fig. 2 (a).

The zero temperature electronic structure and optical properties of carbyne in vacuum on the CAMB3LYP geometry are shown in Fig. 3 (a) and (b). As it can be seen, the CAMB3LYP direct band-gap at zone border is very similar to the one obtained with self-consistent GW (evGW). The optical properties have been calculated using the Bethe-Salpeter equations on top of the evGW eigenvalues. In the absence of quantum anharmonicity, the lowest energy exciton is dark triplet at 2.27 eV, followed by a dark singlet state at 2.55 eV and the bright singlet state at 2.95 eV. The bright singlet exciton corresponds to optical transition across the direct band gap at zone border. However, given the importance of quantum anharmonic effects, a substantial renormalization of the optical gap and optical properties due to vibration occurs in polyyne. We evaluate the effect of quantum anharmonicity on the single particle gap by averaging the density of states over the SSCHA configurations in a 200 atoms polyyne supercell. At $T = 0$, the quantum anharmonic renormalization of the single particle gap is $\approx -0.56$ eV ($\approx 13\%$ of the evGW gap). This is shown in Fig. 3(b), where all the optical spectra are redshifted of the quantum anharmonic renormalization. Thus, we conclude that (i) the effect of quantum-anharmonicity are large and relevant on the optical spectra and (ii) the hybrid functional direct gap is in excellent agreement with Bethe-Salpeter and with that extrapolated from coupled cluster.[4]

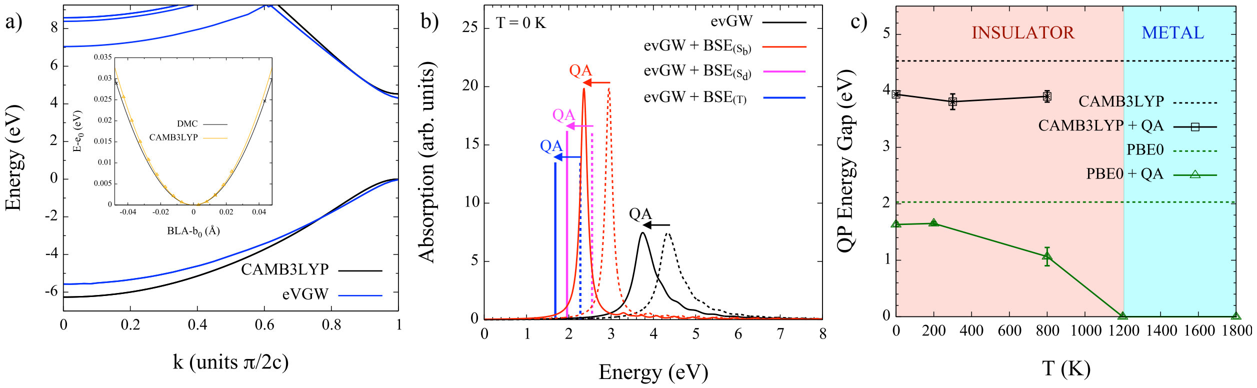

Figure 3: **Insulator to metal transition in polyyne.** a) Electronic structure of polyyne with different approximations for the electron-electron interaction. (b) Optical absorption spectra of carbyne in the Bethe Salpeter approximation on top of evGW with/without inclusion of quantum anharmonic (QA) effects. (c) Quasiparticle band gap in polyyne as a function of temperature computed both with PBE0 and CAMB3LYP functionals, displaying the occurrence of an insulator to metal transition at 1200 K with PBE0.

For what concerns the modeling of Carbyne inside the nanotube, the situation is some-what more complicated as experimental details on the nanotube shape and transport characteristics are missing.[47] As a working hypothesis, we assume the nanotube to be semiconducting and to act as an effective dielectric environment. For what concerns the evGW and Bethe Salpeter calculations on top of the PBE0 geometry, they include the effect of the environment only on the structure but not on the optical spectrum, as they are carried out without explicitly including the nanotube. However, the reduction of the quasiparticle band gap due to the environment can be understood as a polarization effect[49] and therefore treated as an effective dielectric constant,[50] assuming not too strong overlap between the $\pi$ orbitals of the chain and nanotube. A quantitative estimate of the screening of the dielectric environment can be obtained by considering the difference between the evGW (3.21 eV) and PBE (0.93 eV) gaps in the PBE0 geometry, dividing this difference for a typical dielectric constant of an insulator ($\epsilon_M = 3 - 4$) and adding it back to the PBE value. This procedure leads to direct single particle gaps of $1.5 - 1.69$, slightly lower than the PBE0 gap of 2.03 eV. This suggests that the PBE0 single particle gap is of the same order of magnitude as the one obtained in a typical dielectric environment.

Even in this case, quantum-anharmonicity is large and leads to an additional suppression of the band-gap of 0.4 eV, only a factor of 2 smaller than the gap-enhancement found via evGW. However, the effects of quantum anharmonicity strongly increase with temperature. By assuming the evGW correction to the single particle gap to be temperature independent, as it is reasonable to think, we find that the effects of vibrations on the optical gap become dominant at high temperature and lead to a gap closure and a stabilization of a metallic distorted polyynic phase above $T_{MI} \approx 1200$ K (Fig. 3 (c) ) in the presence of an external dielectric environment. This insulator-to-metal transition is then observable and will occur earlier the larger the dielectric constant of the nanotube. In vacuum the larger size of the gap pushes the insulator-metal transition to very large unphysical temperatures, as shown in Fig. 3 (c).

The structural fingerprints of the metallic distorted phase are then a very weak temperature dependence in the BLA and an enhancement of the phonon softening of the optical Raman active mode as a function of temperature, as shown in Fig. 2 (a).

In this work, we have shown that the cumulene-to-polyyne phase transition occurs only at unphysically large temperatures, with a bond length alternation that *increases as temperature increases*. The finite-temperature effects of quantum anharmonicity, poorly explored in literature, are extremely large and strongly affect the structural and vibrational properties as well as the optical absorption. The large band-gap renormalization due to quantum anharmonic effects leads to a completely unexpected insulator-to-metal transition at high temperature stabilising a metallic polyynic phase. The larger the environmental dielectric constant of the nanotube, the lower the temperature for the insulator-metal transition. The experimental synthesis of ultralong polyyne carbon chains[3–5] and temperature dependent optical measurements will allow for an experimental verification of this claim.

# Acknowledgement

D. R. and M.C. acknowledge support from the ANR project ACCEPT (Grant No. ANR-19-CE24-0028). This work was granted access to the HPC resources of IDRIS, CINES and TGCC under the allocation 2021-A0100912417 made by GENCI. Computational resources were also provided by the CINECA award ”ISCRA B” HP10BB2RVB (2019). D. R. thanks D. Varsano for fruitful dicussion on the GW+BSE computations and A. Erba.

# Supporting Information Available

Supporting information accompanies this paper, containing detailed description of: Computational details, SSCHA details, static and dynamic anharmonic phonon spectra of carbyne, ev*GW* electronic structure convergence, CAMB3LYP analysis of polyyne. Correspondence and requests for materials should be addressed to romanin@insp.jussieu.fr and m.calandrabuonaura@unitn.it.

## References

(1) Peierls, R. E. Quelques proprietes typiques des corpses solides. *Ann. I. H. Poincare* **1935**, *5*, 177–222.

(2) Gruner, G. *Density waves in solids*; CRC Press, 1994.

(3) Shi, L.; Rohringer, P.; Wanko, M.; Rubio, A.; Waßerroth, S.; Reich, S.; Cambré, S.; Wenseleers, W.; Ayala, P.; et al. Electronic band gaps of confined linear carbon chains ranging from polyyne to carbyne. *Phys. Rev. Materials* **2017**, *1*, 075601.

(4) Shi, L.; Rohringer, P.; Suenaga, K.; Niimi, Y.; Kotakoski, J.; Meyer, J. C.; Peterlik, H.; Wanko, M.; Cahangirov, S.; Rubio, A. et al. Confined linear carbon chains as a route to bulk carbyne. *Nature Materials* **2016**, *15*, 634–639.

(5) Heeg, S.; Shi, L.; Poulikakos, L. V.; Pichler, T.; Novotny, L. Carbon Nanotube Chirality Determines Properties of Encapsulated Linear Carbon Chain. *Nano Lett.* **2018**, *18*, 5426–5431.

(6) Chalifoux, W. A.; Tykwinski, R. R. Synthesis of polyynes to model the sp-carbon allotrope carbyne. *Nature Chemistry* **2010**, *2*, 967–971.

(7) Agarwal, N. R.; Lucotti, A.; Fazzi, D.; Tommasini, M.; Castiglioni, C.; Chalifoux, W.; Tykwinski, R. R. Structure and chain polarization of long polyynes investigated with infrared and Raman spectroscopy. *J. Raman Spectrosc.* **2013**, *44*, 1398–1410.

(8) da Silva Neto, E. H.; Aynajian, P.; Frano, A.; Comin, R.; Schierle, E.; Weschke, E.; Gyenis, A.; Wen, J.; Schneeloch, J.; Xu, Z. et al. Ubiquitous Interplay Between Charge Ordering and High-Temperature Superconductivity in Cuprates. *Science* **2014**, *343*, 393.

(9) Wilson, J.; Salvo, F. D.; Mahajan, S. Charge-density waves and superlattices in the metallic layered transition metal dichalcogenides. *Advances in Physics* **1975**, *24*, 117–201.

(10) Xi, X.; Zhao, L.; Wang, Z.; Berger, H.; Forró, L.; Shan, J.; Mak, K. F. Strongly enhanced charge-density-wave order in monolayer NbSe2. *Nature Nanotechnology* **2015**, *10*, 765–769.

(11) Chen, Y.; Ruan, W.; Wu, M.; Tang, S.; Ryu, H.; Tsai, H.-Z.; Lee, R.; Kahn, S.; Liou, F.; Jia, C. et al. Strong correlations and orbital texture in single-layer 1T-TaSe2. *Nature Physics* **2020**, *16*, 218–224.

(12) Calandra, M. Charge density waves go nano. *Nature Nanotechnology* **2015**, *10*, 737–738.

(13) Zhang, K.; Liu, X.; Zhang, H.; Deng, K.; Yan, M.; Yao, W.; Zheng, M.; Schwier, E. F.; Shimada, K.; Denlinger, J. D. et al. Evidence for a Quasi-One-Dimensional Charge Density Wave in CuTe by Angle-Resolved Photoemission Spectroscopy. *Phys. Rev. Lett.* **2018**, *121*, 206402.

(14) Zhou, J. S.; Bianco, R.; Monacelli, L.; Errea, I.; Mauri, F.; Calandra, M. Theory of the thickness dependence of the charge density wave transition in 1 T-$TiTe_2$. *2D Materials* **2020**, *7*, 4.

(15) Zhou, J. S.; Bianco, R.; Monacelli, L.; Errea, I.; Mauri, F.; Calandra, M. Anharmonicity and Doping Melt the Charge Density Wave in Single-Layer $TiSe_2$. *Nano Lett.* **2020**, *7*, 4809–4815.

(16) Bianco, R.; Monacelli, L.; Calandra, M.; Mauri, F.; Errea, I. Weak Dimensionality Dependence and Dominant Role of Ionic Fluctuations in the Charge-Density-Wave Transition of $NbSe_2$. *Phys. Rev. Lett.* **2020**, *125*, 106101.

(17) Errea, I.; Calandra, M.; Mauri, F. Anharmonic free energies and phonon dispersions from the stochastic self-consistent harmonic approximation: Application to platinum and palladium hydrides. *Phys. Rev. B* **2014**, *89*, 064302.

(18) Heimann, R. B.; Kleiman, J.; Salansky, N. M. A unified structural approach to linear carbon polytypes. *Nature* **1983**, *306*, 164–167.

(19) Artyukhov, V. I.; Liu, M.; Yakobson, B. I. Mechanically Induced Metal-Insulator Transition in Carbyne. *Nano Lett.* **2014**, *14*, 4224–4229.

(20) Torre, A. L.; Botello-Mendez, A.; Baaziz, W.; Charlier, J.-C.; Banhart, F. Strain-induced metal–semiconductor transition observed in atomic carbon chains. *Nat Commun* **2015**, *6*, 6636.

(21) Romdhane, F. B.; Adjizian, J.-J.; Charlier, J.-C.; Banhart, F. Electrical transport through atomic carbon chains: The role of contacts. *Carbon* **2017**, *122*, 92–97.

(22) Lin, Y.-C.; Morishita, S.; Koshino, M.; Yeh, C.-H.; Teng, P.-Y.; Chiu, P.-W.; Sawada, H.; Suenaga, K. Unexpected Huge Dimerization Ratio in One-Dimensional Carbon Atomic Chains. *Nano Lett.* **2017**, *17*, 494–500.

(23) Milani, A.; Barbieri, V.; Facibeni, A.; Russo, V.; Bassi, A. L.; Lucotti, A.; Tommasini, M.; Tzirakis, M. D.; Diederich, F.; Casari, C. S. Structure modulated charge transfer in carbon atomic wires. *Sci Rep* **2019**, *9*, 1648.

(24) Malard, L. M.; Nishide, D.; Dias, L. G.; Capaz, R. B.; Gomes, A. P.; Jorio, A.; Achete, C. A.; Saito, R.; Achiba, Y.; Shinohara, H. et al. Resonance Raman study of polyynes encapsulated in single-wall carbon nanotubes. *Phys. Rev. B* **2007**, *76*, 233412.

(25) Moura, L. G.; Malard, L. M.; Carneiro, M. A.; Venezuela, P.; Capaz, R. B.; Nishide, D.; Achiba, Y.; Shinohara, H.; Pimenta, M. A. Charge transfer and screening effects in

polyynes encapsulated inside single-wall carbon nanotubes. *Phys. Rev. B* **2009**, *80*, 161401(R).

(26) Fantini, C.; Cruz, E.; Jorio, A.; Terrones, M.; Terrones, H.; Lier, G. V.; Charlier, J.-C.; Dresselhaus, M. S.; Saito, R.; Kim, Y. A. et al. Resonance Raman study of linear carbon chains formed by the heat treatment of double-wall carbon nanotubes. *Phys. Rev. B* **2006**, *73*, 193408.

(27) Andrade, N. F.; Vasconcelos, T. L.; Gouvea, C. P.; Archanjo, B. S.; Achete, C. A.; Kim, Y. A.; Endo, M.; Fantini, C.; Dresselhaus, M. S.; Filho, A. S. Linear carbon chains encapsulated in multiwall carbon nanotubes: Resonance Raman spectroscopy and transmission electron microscopy studies. *Carbon* **2015**, *90*, 172–180.

(28) Bianco, R.; Errea, I.; Paulatto, L.; Calandra, M.; Mauri, F. Second-order structural phase transitions, free energy curvature, and temperature-dependent anharmonic phonons in the self-consistent harmonic approximation: Theory and stochastic implementation. *Phys. Rev. B* **2017**, *96*, 014111.

(29) Monacelli, L.; Errea, I.; Calandra, M.; Mauri, F. Pressure and stress tensor of complex anharmonic crystals within the stochastic self-consistent harmonic approximation. *Phys. Rev. B* **2018**, *98*, 024106.

(30) Monacelli, L.; Bianco, R.; Cherubini, M.; Calandra, M.; Errea, I.; Mauri, F. The stochastic self-consistent harmonic approximation: calculating vibrational properties of materials with full quantum and anharmonic effects. *J. Phys.: Condens. Matter* **2021**, *33*, 363001.

(31) Giannozzi, P.; Baroni, S.; Bonini, N.; Calandra, M.; Car, R.; Cavazzoni, C.; Ceresoli, D.; Chiarotti, G. L.; Cococcioni, M.; Dabo11, I. et al. QUANTUM ESPRESSO: a modular and open-source software project for quantum simulations of materials. *Journal of Physics: Condensed Matter* **2009**, *21*, 395502.

(32) Giannozzi, P.; Andreussi, O.; Brumme, T.; Bunau, O.; Nardelli, M. B.; Calandra, M.; Car, R.; Cavazzoni, C.; Ceresoli, D.; Cococcioni, M. et al. Advanced capabilities for material modeling with Quantum ESPRESSO. *Journal of Physics: Condensed Matter* **2017**, *29*, 465901.

(33) Dovesi, R.; Orlando, R.; Erba, A.; Zicovich-Wilson, C. M.; Civalleri, B.; Casassa, S.; Maschio, L.; Ferrabone, M.; Pierre, M. D. L.; D'Arco, P. et al. Crystal14: A program for the ab-initio investigation of crystalline solids. *International Journal of Quantum Chemistry* **2014**, *114*, 1287–1317.

(34) Dovesi, R.; Erba, A.; Orlando, R.; Zicovich-Wilson, C. M.; Civalleri, B.; Maschio, L.; Rérat, M.; Casassa, S.; Baima, J.; Salustro, S. et al. Quantum-mechanical condensed matter simulations with CRYSTAL. *WIREs Comput Mol Sci.* **2018**, *8*, 1360.

(35) Oliveira, D. V.; Laun, J.; Peintinger, M. F.; Bredow, T. Bsse-correction scheme for consistent gaussian basis sets of double- and triple-zeta valence with polarization quality for solid-state calculations. *Journal of Computational Chemistry* **2019**, *40*, 2364–2376.

(36) Marini, A.; Hogan, C.; Grüning, M.; Varsano, D. yambo: An ab initio tool for excited state calculations. *Computer Physics Communications* **2009**, *8*, 180.

(37) Sangalli, D.; Ferretti, A.; Miranda, H.; Attaccalite, C.; Marri, I.; Cannuccia, E.; Melo, P.; Marsili, M.; Paleari, F.; Marrazzo, A. et al. Many-body perturbation theory calculations using the yambo code. *Journal of Physics: Condensed Matter* **2019**, *31*, 325902.

(38) Rojas, H. N.; Godby, R. W.; Needs, R. J. Space-Time Method for Ab Initio Calculations of Self-Energies and Dielectric Response Functions of Solids. *Phys. Rev. B* **1995**, *74*, 10.

(39) Strinati, G. Application of the Green's functions method to the study of the optical properties of semiconductors. *Rivista del Nuovo Cimento* **1988**, *11*, 12.

(40) Bussi, G. Effects of the Electron–Hole Interaction on the Optical Properties of Materials: the Bethe–Salpeter Equation. *Physica Scripta* **2003**, *2004*, 141.

(41) Abdurahman, A.; Shukla, A.; Dolg, M. Ab initio many-body calculations on infinite carbon and boron-nitrogen chains. *Phys. Rev. B* **2002**, *65*, 115106.

(42) Yang, S.; Kertesz, M. Bond Length Alternation and Energy Band Gap of Polyyne. *J. Phys. Chem. A* **2006**, *110*, 9771–9774.

(43) Jacquemin, D.; Femenias, A.; Chermette, H.; Ciofini, I.; Adamo, C.; André, J.-M.; Perpète, E. A. Assessment of Several Hybrid DFT Functionals for the evaluation of Bond Length Alternation of Increasingly Long Oligomers. *J. Phys. Chem. A* **2006**, *110*, 5952–5959.

(44) Peach, M. J. G.; Tellgren, E. I.; Salek, P.; Helgaker, T.; ; Tozer, D. J. Structural and Electronic Properties of Polyacetylene and Polyyne from Hybrid and Coulomb-Attenuated Density Functionals. *J. Phys. Chem. A* **2007**, *111*, 11930–11935.

(45) Mostaani, E.; Monserrat, B.; Drummond, N. D.; Lambert, C. J. Quasiparticle and excitonic gaps of one-dimensional carbon chains. *Phys. Chem. Chem. Phys.* **2016**, *18*, 14810–14821.

(46) Ramberger, B.; Kresse, G. New insights into the 1D carbon chain through the RPA. *Phys. Chem. Chem. Phys.* **2021**, *23*, 5254.

(47) Experimentally it is unclear if the double wall nanotubes into which carbyne is grown are insulating or metallic as the chains are grown inside the inner tubes at very high temperature from filled carbonaceous precursors.

(48) Shi, L.; Rohringer, P.; Wanko, M.; Rubio, A.; Waßerroth, S.; Reich, S.; Cambré, S.; Wenseleers, W.; Ayala, P.; Pichler, T. Electronic band gaps of confined linear carbon chains ranging from polyyne to carbyne. *Phys. Rev. Materials* **2017**, *1*, 075601.

(49) Neaton, J. B.; Hybertsen, M. S.; Louie, S. G. Renormalization of Molecular Electronic Levels at Metal-Molecule Interfaces. *Phys. Rev. Lett.* **2006**, *97*, 216405.

(50) Nugraha, A. R. T.; Saito, R.; Sato, K.; Araujo, P. T.; Jorio, A.; Dresselhaus, M. S. Dielectric constant model for environmental effects on the exciton energies of single wall carbon nanotubes. *Appl. Phys. Lett.* **2010**, *97*, 091905.